Appl. Phys. B 70, 345–349 (2000) / Digital Object Identifier (DOI) 10.1007/s003409900175

Applied Physics B
Lasers
and Optics

Tm,Ho:YLF microchip laser under Ti:sapphire and diode pumping

G.L. Bourdet, R.A. Muller

Laboratoire d'Optique Appliquée, Ecole Polytechnique, Ecole Nationale Supérieure de Techniques Avancées, CNRS UMR 7639, Chemin de la Hunière, 91761 Palaiseau Cedex, France
(E-mail: bourdet@enstay.ensta.fr)

Received: 19 June 1999/Revised version: 2 August 1999/Published online: 30 November 1999

Abstract. In this paper, we compare the performances of a Tm,Ho:YLF microchip laser when pumped by a Ti:sapphire laser and by a fiber-coupled diode laser. We report the performances obtained for both pumping schemes. Afterwards, we analyse, the reasons for the reduction in efficiency. Using a theoretical model, we conclude that the loss in performance for diode pumping is essentially due to the pump power reflected by the laser cavity when the crystal faces present parasitic reflectivity at the pump wavelength.

PACS: 42-55.Xi

Co-doped Tm,Ho lasers received a large amount of interest during the ten past years. These lasers seem to be the best candidates for a wide range of applications including medicine [1] and eye-safe remote sensing systems [2]: laser ranging, coherent Doppler lidar for wind sensing, wind-shear detection, DIAL water vapour profiling, etc. Thereby, they received a large attention from the space and aviation agencies for both cw master oscillator [3–6] or powerful transmitters [7–12]. In previous papers [13, 14], we have derived a complete theoretical model making it possible to forecast the performances of a microchip laser taking into account the ground-state depletion, the up-conversion, and the amount of pump power stored in the laser cavity resulting from the reflectivity of the laser mirrors at pump wavelength. The validity of this model has been checked with Tm^{3+}:YVO_4 [13] and Tm,Ho:YLF [14] under Ti:sapphire pumping and good agreement between the theoretical predictions and the experimental results has been found. We now compare the performances obtained with Ti:sapphire and diode pumping. We first analyse the results of a Ti:sapphire-pumped Tm,Ho:YLF microchip laser under various experimental conditions including the pump beam size, the crystal temperature, and the angle between the pump light polarisation and the crystal axis. We then report the results obtained using the same microchip laser with fiber-coupled diode pumping. For 1.2 W pump power, overall efficiency as large as 42% and 27% has been obtained with Ti:sapphire and diode pumping, respectively. This reduction in efficiency is analysed and we find that, in addition of the reduction due to the random polarisation of the pump light and the mis-match of the diode and absorption linewidth for diode pumping, the residual reflectivity of the crystal faces at the pump wavelength plays a different role for Ti:sapphire and diode pumping. Although it may be favourable for storing more pump power for Ti:sapphire laser pumping, the linewidth of which is small with respect to the free spectral range of the laser cavity, it is prejudicial for diode pumping for which the linewidth is larger than the free spectral range and then, a larger amount of the launched pump power is reflected by the laser.

1 Ti:sapphire pumping

The experimental set-up used (Fig. 1) is identical to the one described in [14]. The microchip laser is made of an *a*-cut 6% Tm, 0.4% Ho YLF crystal 2.5 mm in length. The faces are polished plane and parallel. This crystal is set in an active mirror configuration in which the rear face, high-reflectivity-coated for both pump (792 nm) and laser (2060 nm) wavelengths, is bonded with a conductive glue on a heat sink. The pump beam is injected by means of a dichroïc mirror which reflects the pump beam and transmits the laser beam. The pump polarisation is parallel to the crystal *c* axis. The reflectivity of the front face at laser wavelength is 98%, whereas its transmissivity at pump wavelength is larger than 85%. Preliminary experiments [14] have shown that this transmissivity is about 92%. The injected pump power is varied using a halfwave plate followed by a polariser and it is monitored using the fraction (3%) transmitted by the dichroïc mirror making it possible to control possible backcoupling of the pump light reflected by the microchip laser into the pump source. As shown in [13] and [14], the cavity can store or reject an amount of the launched pump power when the crystal faces exhibit an unwanted reflectivity at the pump wavelength. In order to hold the cavity in resonance with the pump wavelength, it is necessary to adjust the crystal axis with respect to the pump beam direction. The tilt angle leading to maximum output power is approximately equal to 1.5° making it possible to avoid unwanted feedback in the pump laser.

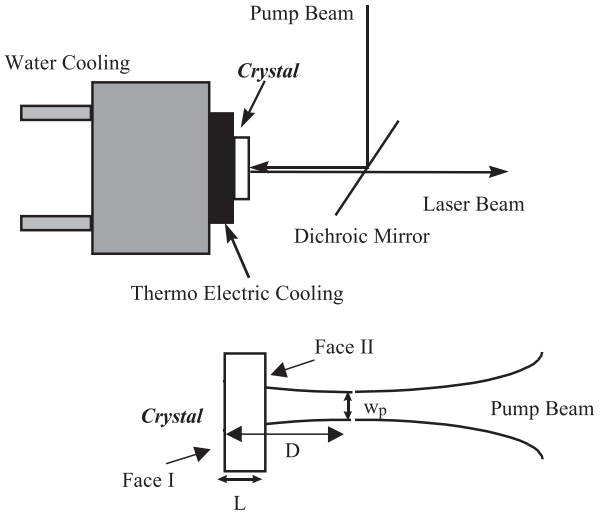

Fig. 1. Experimental set-up

We have experimentally found that this adjustment is stable after a short time of heating and that it does not largely depend on the injected pump power resulting from the cooling efficiency of the active mirror configuration. In a first step, we measure the laser performances versus the pump beam size. In Fig. 2, the threshold and the slope efficiency for a pump beam size ranging from 25 μm to 96 μm appear. These results show that the performances are not very dependent upon the pump beam size between 50 μm and 96 μm. Setting the pump beam size equal to its optimum value (75 μm), we have measured the laser output power versus the launched pump power when the heat sink temperature is varied. The results are plotted in Fig. 3.

In a second step, and for a pump power of 1.2 W, we investigate the variations of the output power versus the angle between the polarisation of the pump light and the *c* axis of the crystal. The results are plotted in Fig. 4. The ratio of

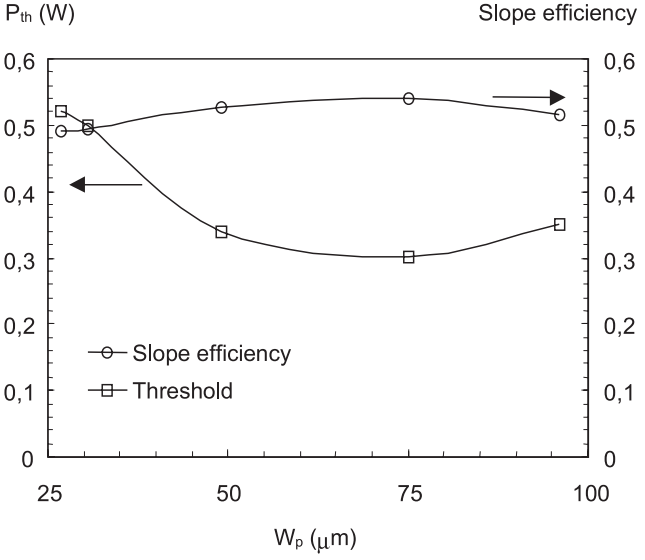

Fig. 2. Threshold (*squares*, *left scale*) and slope efficiency (*circles*, *right scale*) versus pump beam size

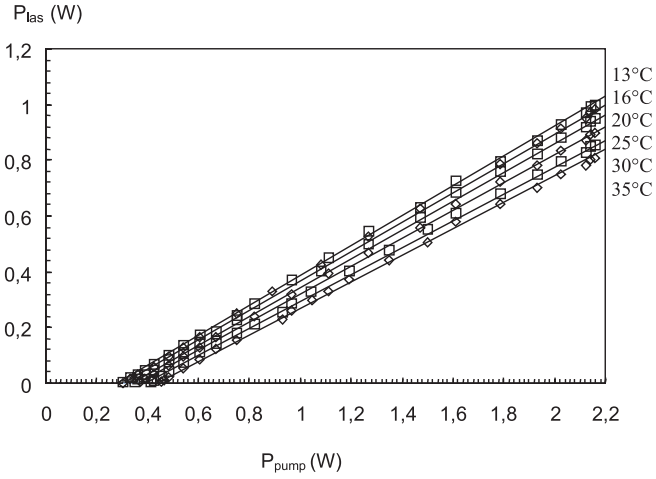

Fig. 3. Laser output power versus launched pump power for various heat sink temperatures

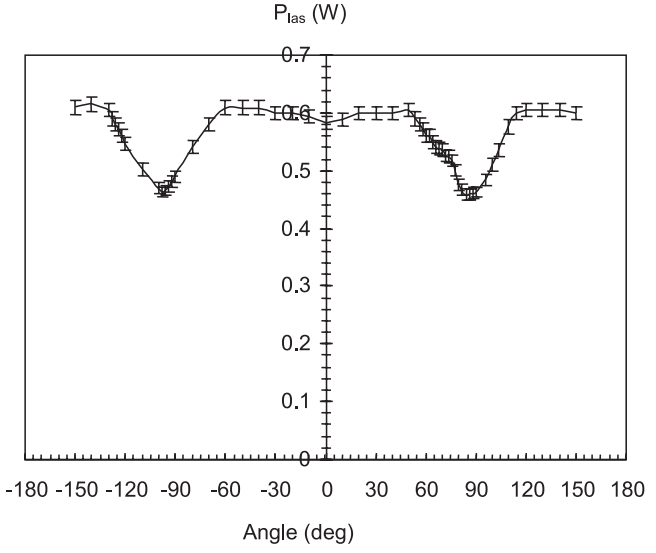

Fig. 4. Laser output power versus the tilt angle between the pump light polarisation and the crystal *c* axis for 1.2 W launched pump power

the output power for both perpendicular and parallel pump polarisations with respect to the crystal *c* axis is 74%, in good agreement with 76% computed using the model described in [14]. It may appear surprising that the laser output power when the crystal is pumped following the *a* axis is only 26% lower than the one supplied when pumped following the *c* axis with regards to the difference between the absorption coefficients for both directions (3.2 cm^{-1} and 5.4 cm^{-1}, respectively). However, we must take into account the nonlinear coupling between the gain and the absorption in the amplifier medium. We note that the laser light polarisation is always parallel to the crystal *c* axis and that the mean output power is 92% of the maximum when the angle is varied.

2 Diode pumping

We now investigate diode pumping. The diode we used is a fibre-coupled single diode (Opto Power Corp. A002FC150)

capable of supplying 1.2 W through a multimode fibre. This fibre has a core diameter of 150 μm and the total divergence is 16°. Using two confocal lenses 10 cm in focal length, the image of the fibre output is made in the microchip. In order to ensure that the diode wavelength is in resonance with the crystal absorption line (792 μm), the diode temperature is tuned when the diode current is varied. In Fig. 5 the intensity distribution focused by the optical system for both horizontal (upper curve) and vertical (lower curve) directions appears. We note that the shape is quasi-Gaussian with a waist size equal to 96 μm. In Fig. 6 the spot size in both horizontal and vertical directions is plotted versus the distance when the crystal is translated along the direction of the pump beam. This shows that the pump beam size, once corrected for the effect of the refractive index equal to 1.47 for YLF, undergoes small variations when it propagates in the 2.5-mm-long crystal (96 μm to 120 μm). The position refers to the rear face of the crystal. Also shown in this figure is the corresponding laser output power whose maximum value is reached when the pump beam waist is set on the rear face of the crystal. We notice that the same experiment performed with Ti:sapphire pumping with a 96-μm waist size shows that the output power variation around its optimal value is only 4% for a translation length of ±10 mm. Figure 7 shows the output power versus the launched pump power for various heat sink temperatures. On the other hand, we note that the orientation of the crystal with respect to the pump beam is not very sensitive (10° for 10% fall in output power) and that the reflected pump power does not affect the injected pump power when a small tilt angle is set. In Fig. 8 the pump threshold P_{th} (circles) and the slope efficiency (squares) versus the crystal temperature for both Ti:sapphire pumping with a pump beam waist equal to 75 μm (open) and diode pumping (filled) for 1.2-W pump power are plotted.

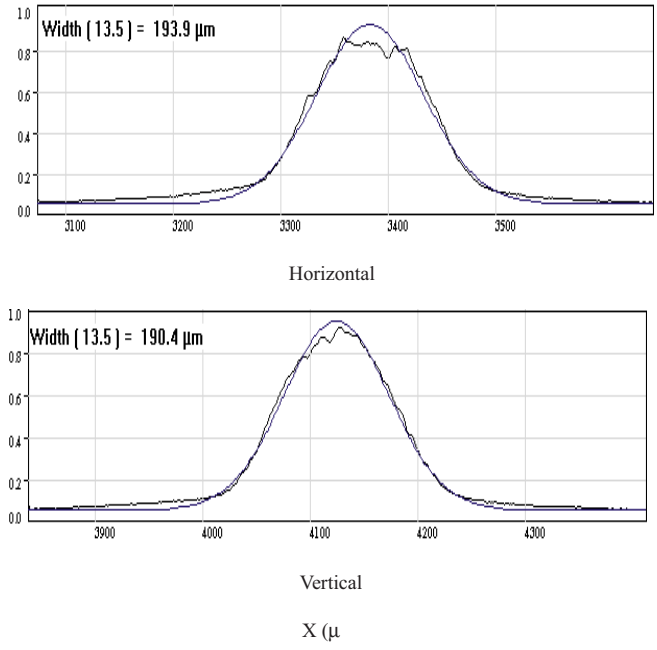

Fig. 5. Cross section of the focused beam supplied by the fibre-coupled diode for 1.2 W output power

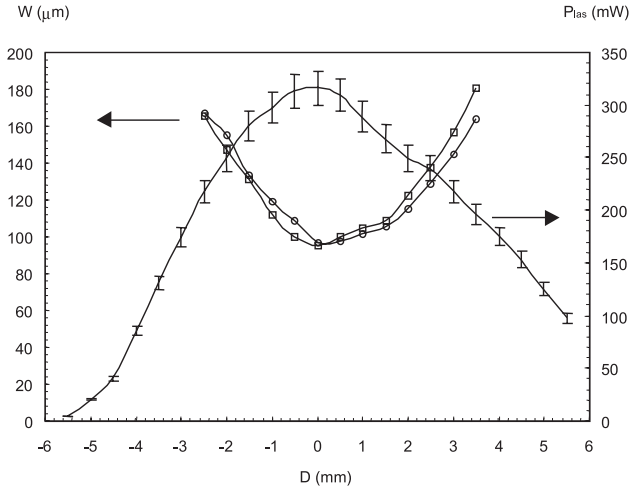

Fig. 6. Beam size of the focused beam supplied by the fibre-coupled diode versus distance (□ *horizontal*, ○ *vertical*, *left scale*) and corresponding laser output power (*right scale*) for 1.2 W pump power

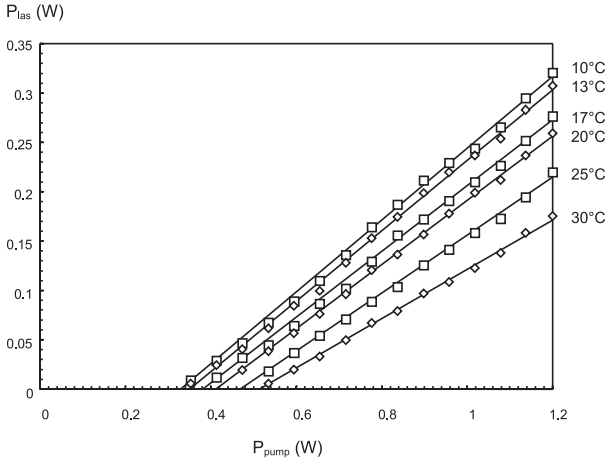

Fig. 7. Laser output power versus launched pump power when diode pumped for various temperatures of the heat sink

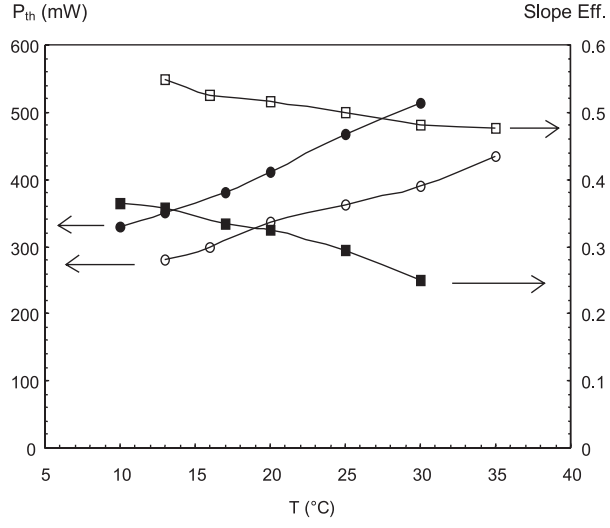

Fig. 8. Pump threshold (*circles*, *left scale*) and slope efficiency (*squares*, *right scale*) versus heat sink temperature for laser (*open*) and diode (*filled*) pumping

3 Discussion

Three processes may be responsible of the loss in performances for diode pumping compared to those obtained with Ti:sapphire pumping. The first is the pump beam mismatching. This may play a dominant role for direct diode pumping for which the output beam is notorious for aberrated and astigmatic profiles. However, with regards to Figs. 5 and 6, it does not seem of great importance with a fibre-coupled diode. The second is the mis-match between the pump spectrum and the absorption line. In this case, the loss in the pump efficiency may be worsened when the laser mirrors have an unwanted reflectivity at the pump wavelength. As the front mirror is not perfectly transparent at the pump wavelength ($R = 8\%$), the laser cavity will store more pump power for the resonant wavelength and the non-resonant wavelengths will be reflected. In [13], it is shown that the pump intensity absorbed when the laser is above threshold reads:

$$I_{\mathrm{abs}} = \frac{\left(1-R_{\mathrm{s}}^{\mathrm{p}}\right)\left(1+\sqrt{\Gamma R_{\mathrm{m}}^{\mathrm{p}}}\right)\left(1-\sqrt{\frac{\Gamma}{R_{\mathrm{m}}^{\mathrm{p}}}}\right)}{1+R_{\mathrm{s}}^{\mathrm{p}}\Gamma-2\sqrt{R_{\mathrm{s}}^{\mathrm{p}}\Gamma}\cos\varphi} I_{\mathrm{inj}} \,, \tag{1}$$

where I_{inj} is the launched pump intensity, $R_{\mathrm{s}}^{\mathrm{i}}$ and $R_{\mathrm{m}}^{\mathrm{i}}$ are the output and rear mirror reflectivity, respectively, for the pump ($\mathrm{i} = \mathrm{p}$) and the laser ($\mathrm{i} = \mathrm{l}$), φ the change of phase undergone by the pump wave for a round trip in the cavity and:

$$\Gamma = R_{\mathrm{m}}^{\mathrm{p}}(R_{\mathrm{s}}^{\mathrm{l}}R_{\mathrm{m}}^{\mathrm{l}})^{-D}\mathrm{e}^{-2\delta L_{\mathrm{c}}} \,, \qquad D = \frac{\alpha_0}{g_0}\frac{\xi^2}{\theta} \,,$$

$$\delta = \alpha_0\xi(1-f) \,, \qquad \xi = \frac{1}{1-f\frac{\theta-1}{\theta}} \,, \qquad f = \frac{f_{\mathrm{l}}}{f_{\mathrm{u}}+f_{\mathrm{l}}} \,.$$

L_{c} is the laser length, Γ is the round-trip transmission in the cavity taking into account the reflection by the rear mirror and the absorption of the crystal, f_{u} and f_{l} are the Boltzmann factors of the upper and lower levels of the lasing transition, respectively, θ is the energy transfer parameter defined in [14] and:

$$g_0 = \sigma_{\mathrm{l}}N_{\mathrm{Ho}}(f_{\mathrm{u}}+f_{\mathrm{l}}) \,, \qquad \alpha_0 = \sigma_{\mathrm{p}}N_{\mathrm{Tm}} \,,$$

σ_{i} is the emission ($\mathrm{i} = \mathrm{l}$) and absorption ($\mathrm{i} = \mathrm{p}$) cross section and N_{j} is the concentration of Thulium ($\mathrm{j} = \mathrm{Tm}$) and Holmium ($\mathrm{j} = \mathrm{Ho}$), respectively.

For Ti:sapphire pumping, the stored intensity has been summed over the Ti:sapphire oscillating modes. For diode pumping, it must be integrated over the diode spectrum. In both cases, we take into account the dependence on wavelength of the parameters. The amount of the injected pump intensity stored in the cavity then reads:

$$A = \frac{\int \frac{\left(1-R_{\mathrm{s}}^{\mathrm{p}}\right)\left(1+\sqrt{\Gamma(\lambda)R_{\mathrm{m}}^{\mathrm{p}}}\right)\left(1-\sqrt{\frac{\Gamma(\lambda)}{R_{\mathrm{m}}^{\mathrm{p}}}}\right)}{1+R_{\mathrm{s}}^{\mathrm{p}}\Gamma(\lambda)-2\sqrt{R_{\mathrm{s}}^{\mathrm{p}}\Gamma(\lambda)}\cos\varphi(\lambda)} I_{\mathrm{inj}}(\lambda)\mathrm{d}\lambda}{\int I_{\mathrm{inj}}(\lambda)\mathrm{d}\lambda} \,. \tag{2}$$

In order to compute the amount of launched pump power absorbed by the crystal, we assume an absorption line FWHM of 3 nm and 16 nm for a polarisation parallel to the c and the a axis, respectively [6] and:

$$g_0 = 0.94\,\mathrm{cm}^{-1} \,, \qquad L_{\mathrm{c}} = 0.25\,\mathrm{cm} \,,$$
$$P//c: \qquad \alpha_0 = 5.4\,\mathrm{cm}^{-1} \,, \qquad n = 1.473 \,,$$
$$P//a: \qquad \alpha_0 = 3.2\,\mathrm{cm}^{-1} \,, \qquad n = 1.450 \,,$$
$$T = 15\,^{\circ}\mathrm{C} \,, \qquad f = 0.21 \,, \qquad f_{\mathrm{u}}+f_{\mathrm{l}} = 0.11 \,, \qquad \theta = 18 \,,$$
$$R_{\mathrm{s}}^{\mathrm{l}} = 0.98 \,, \qquad R_{\mathrm{s}}^{\mathrm{p}} = 0.08 \,, \qquad R_{\mathrm{m}}^{\mathrm{l}} = R_{\mathrm{m}}^{\mathrm{p}} = 0.995 \,.$$

On the other hand, the diode spectrum is 3 nm FWHM and the Ti:sapphire spectrum is made of 140 modes spaced by 150 MHz free spectral range (FWHM of 3.2×10^{-2} nm). In Fig. 9, the results for Ti:sapphire pumping (open squares) when the pump polarisation is parallel to the crystal c axis and for diode pumping (open and filled circles for the pump polarisation parallel to the c and the a axis, respectively, and crosses for the mean value) versus the reflectivity of the crystal front face at the pump wavelength are plotted. In both cases, the central wavelength of the pump has been assumed to be in resonance with the laser cavity. It should be pointed out that the stored pump power reaches a maximum for Ti:sapphire with resonant pumping whereas it always decreases for diode pumping. This may be easily understood considering that the free spectral range of the laser cavity (0.87 nm) is larger than the FWHM of the Ti:sapphire laser (0.032 nm) but smaller than the one of the diode (3 nm). Then, Ti:sapphire pumping should be more efficient with a proper front-face reflectivity and resonant pumping. Nevertheless, as a result of the pump linewidth with respect to the crystal absorption linewidth, Ti:sapphire pumping should be always more efficient than diode pumping, even with a perfect transmission of the front-face mirror at pump wavelength. In this case, the amount of stored pump power is 93% for Ti:sapphire pumping following the c axis, whereas it is 86% and 78% for diode pumping following the c and a axis, respectively. For a front-face reflectivity at pump wavelength of 8%, the mean value of the stored pump power averaged over the two pump polarisations is 76% for diode pumping

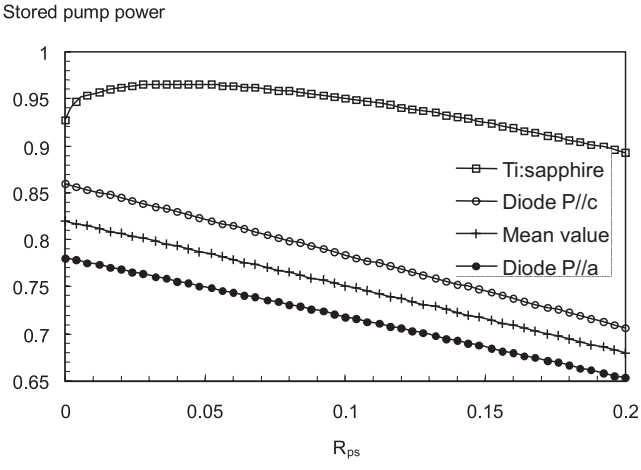

Fig. 9. Stored amount of the launched pump power versus reflectivity of the front face of the crystal at the pump wavelength for resonant Ti:sapphire (*squares*) and diode (*open* and *filled circles* for the pump polarisation parallel and perpendicular to the c axis, respectively, and crosses for the mean value) pumping

when it reaches 96% for resonant Ti:sapphire pumping with a polarisation parallel to the *c* axis.

The last process responsible of the drop in efficiency is the effect of the random polarisation of the light supplied by the fibre-coupled diode with respect to the birefringence of the laser crystal.

Figure 10 shows the laser output power for Ti:sapphire pumping (squares) and for diode pumping (circles) with a pump beam size of 96 μm in both cases versus the theoretical absorbed pump power computed using the former relations. The experimental data concerning Ti:sapphire pumping have been reduced by a factor of 92% for comparison with those obtained with random-polarisation diode pumping. We then obtain a threshold of 0.27 W for both Ti:sapphire and diode pumping with almost equal slope efficiency (51% against 49%). With regard to these results, we can estimate that the difference in divergence between the two pump sources is not of great importance in our case. This may be understood considering that, as the laser mode is always wider than the pump mode, a fraction of the laser mode travels through unpumped regions for a low divergent pump beam (Ti:sapphire) when it may be amplified with a higher divergent pump source (diode). Then, the effect of the divergence may be compensated. We then conclude that one of the main effects responsible for the decrease in pump efficiency between Ti:sapphire and diode pumping is the reflected pump light that is larger for diode pumping than for laser pumping when the laser cavity front-face mirror reflects the pump beam.

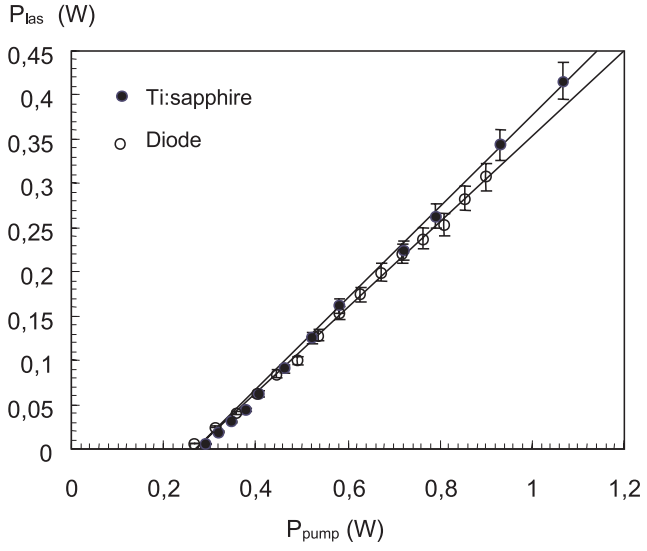

Fig. 10. Laser output power versus theoretical absorbed pump power for Ti:sapphire (*squares*) and diode (*circles*) pumping. Data of Ti:sapphire pumping have been corrected in order to take into account the random polarisation of the diode light

4 Conclusion

We have presented experimental results obtained with a Tm, Ho:YLF microchip laser when Ti:sapphire and diode pumped. Overall efficiency as large as 42% has been obtained with Ti:sapphire laser pumping with 1.2 W (46% for 2.1 W). On the other hand, the effect of the direction of the pump light polarisation with respect to the *c* axis of the crystal does not affect dramatically the laser efficiency in our case. Last, we have investigated the reduction in efficiency when the microchip is pumped with a fibre-coupled diode. We find that this reduction is mainly dominated by the effect of the reflectivity of the front face at the pump wavelength. Then, resonant pumping with Ti:sapphire laser for which the linewidth is smaller than the free spectral range of the laser cavity occurs instead of diode pumping, for which the linewidth is larger than the free spectral range resulting in a large reflection of launched pump power.

References

1. N.S. Mishioka, Y. Damakevitz: IEEE J. Quantum Electron. **QE-26**, 2271 (1990)
2. S.W. Henderson, P.J.M. Suni, C.P. Hale, S.M. Hannon, J.R. Magee, D.L. Bruns, E.H. Yuen: IEEE Trans. Geosci. Remote Sensing **31**, 4 (1993)
3. B.T. McGuckin, R.T. Menzies: IEEE J. Quantum Electron. **QE-28**, 1025 (1992)
4. B.T. McGuckin, R.T. Menzies, C. Esproles: Appl. Opt. **32**, 2082 (1993)
5. G.J. Koch, J.P. Deyst, M.E. Storm: Opt. Lett. **18**, 1235 (1993)
6. I.F. Elder, M.J.P. Payne: Opt. Commun. **145**, 329 (1998)
7. N.P. Barnes, E.D. Filer, C.A. Morrison, C.J. Lee: IEEE J. Quantum Electron. **QE-32**, 92 (1996)
8. C.J. Lee, G. Han, N.P. Barnes: IEEE J. Quantum Electron. **QE-32** 105 (1996)
9. M.G. Jani, N.P. Barnes, K.E. Murray, G.E. Lockard: Opt. Lett. **18**, 1636 (1993)
10. M.G. Jani, N.P. Barnes, K.E. Murray: Appl. Opt. **36**, 3357 (1997)
11. N.P. Barnes, K.E. Murray, M.G. Jani: Appl. Opt. **36**, 3363 (1997)
12. D. Bruneau, S. Delmonte, J. Pelon: Appl. Opt. **37**, 8406 (1998)
13. G.L. Bourdet, G. Lescroart: Opt. Commun. **149**, 404 (1998)
14. G.L. Bourdet, G. Lescroart: Appl. Opt. **38**, 3275 (1999)
15. G.L. Bourdet, G. Lescroart, R. Muller: Opt. Commun. **150**, 141 (1998)